Molecular Models for the Intercalation of Methane Hydrate Complexes in Montmorillonite Clay

Randall T. Cygan,*,† Stephen Guggenheim,‡ and August F. Koster van Groos‡

Geochemistry Department, Sandia National Laboratories, Albuquerque, New Mexico 87185-0750 and Department of Earth and Environmental Sciences, University of Illinois at Chicago, Chicago, Illinois 60607-7059

Molecular simulations were performed to determine the structure and behavior of methane and H_2O in the interlayer of various montmorillonite clays. Molecular dynamics using NPT ensembles and large simulation supercells—comprised of Na-, K-, Ca-, and Mg-montmorillonite with methane and H_2O—provide all-atom trajectories for simulation times up to 200 ps. Simulated X-ray diffraction patterns for the equilibrated structures exhibit basal (001) *d*-values that range from 23 Å to 24 Å. Radial distribution functions for carbon−carbon, oxygen−oxygen, and carbon−oxygen derived from the trajectories indicate an interlayer structure that is different from the bulk methane hydrate and from methane in aqueous solution. Some order of the methane hydrate structure is preserved within the interlayer and is related to the formation of methane clathrate structures with H_2O and the clay surfaces and the formation of a hydrogen-bonded network in the interlayer. The theoretical results support the recent experimental observation of a stable methane hydrate intercalate with Na-montmorillonite.

Introduction

There is much unknown about the interaction of methane and clays. Recently, experimental evidence for the formation of smectite that accommodates methane hydrate in the regions between the 2:1 (silicate) layers was presented by Guggenheim and Koster van Groos;[1] they succeeded in intercalating methane hydrate and the 2:1 layers of Na-exchanged montmorillonite. Other workers, for example, Cha et al.,[2] showed the importance of large specific surface areas in the nucleation of gas hydrates. Thus, the presence of clays, which involve large specific surface areas, would be expected to aid in the formation of gas hydrates.

Because of the limited experimental data and information about natural samples, computational chemistry and computer modeling have been used to obtain information about possible ways to incorporate methane in smectite.[3−6] These studies, however, did not use a starting model involving methane hydrate intercalated between 2:1 layers. Instead, it was assumed that methane molecules could be accommodated in a two-water layer interlayer[3] or that the analysis involved a model where methane molecules were solvated by 12−13 H_2O molecules and 8 oxygen atoms of the clay siloxane surface to obtain a distorted 20-fold site about CH_4.[4]

Guggenheim and Koster van Groos[1] described experiments that place constraints on the structure of the intercalated methane hydrate between the 2:1 layers of the montmorillonite: (1) The montmorillonite−methane hydrate intercalate phase decomposes at conditions in temperature and pressure that are similar to those of methane hydrate[7] resulting in montmorillonite plus methane hydrate. This result suggests that methane hydrate exists in the interlayer region of the clay; (2) the intercalate phase is characterized by a strong ∼22 Å peak and a weak second-order

∼11 Å reflection in oriented clay aggregate X-ray diffraction mounts, not only suggesting the intercalation of ∼12 Å hydrate[8] within the ∼9.8 Å silicate layers but also considerable disorder between the layers; (3) in low-temperature studies at one atmosphere, Ahlrichs and White[9] and Anderson and Morganstern[10] showed that montmorillonite in the presence of water collapses to a *d*(001) value of ∼19 Å upon freezing and to ∼16 Å at −10°C. Similarly, at less than −8.5°C and ∼40 atm methane pressure, the interlayer material in the montmorillonite−methane hydrate intercalate phase is destabilized, and the structure collapses to a *d*(001) spacing of ∼16 Å. In contrast, methane hydrate is not known to be unstable at these lower temperatures. This result suggests that H_2O molecules present in the interlayer destabilizes the montmorillonite−methane hydrate intercalate phase. These H_2O molecules must be relatively independent from the hydrate portion of the intercalate.

In this paper, we report on the modeling of the montmorillonite−methane hydrate intercalate by computational chemistry methodologies. Unlike previous modeling approaches where information about methane adsorption in clay was limited, we use the information from the experimental work to guide the development of the models. Molecular simulation methods have previously been used to examine the structure and phase equilibria of various gas hydrates, but none have examined the complex interactions between clay and the gas hydrate intercalate. In an effort to better understand gas hydrate stability, Rodger[11] and Rodger et al.[12] performed molecular dynamics (MD) simulations of small methane hydrate systems on the basis of simple host−water interaction models. More detailed dynamics modeling of the methane hydrate were completed by Hwang et al.[13] and Forrishahl et al.[14] to better simulate the distortion of the host lattice by the guest molecule. More rigorous models using isobaric−isothermal ensembles (NPT) and allowing fully flexible H_2O were introduced by Zele et al.[15] where the guest

molecules were represented as groups of rigid atoms. Recently, Chialvo et al.[16] performed a series of NPT ensemble simulations of the methane and carbon dioxide hydrates using three different rigid H_2O models to obtain greater variations in structure and energy. These previous computational studies are noteworthy in their ability to provide the atomistic details associated with guest−host interactions that control the hydrate phase equilibria. Previously a statistical thermodynamic model[17] was used with limited success to describe gas hydrate phase relations.

Recent efforts in the development of accurate energy force fields for the molecular simulation of clay minerals[18−20] have led to significant advances in evaluating the structure of clay minerals and the energetics of processes involving clays. Owing to the small particle size of clays (often in nanometer ranges), the lack of stacking disorder, complex multicomponent compositions, and defect structures, molecular simulations provide a convenient method for obtaining insights into atomic structure and behavior. X-ray diffraction refinements of crystal structures for clay minerals are limited to only clay minerals where samples exist of sufficient particle size and atomic order to obtain near ideal (Bragg) diffraction.[21,22] Computational methods have apparently succeeded in analyzing various clay minerals,[18,20] the swelling behavior of smectite,[23,24] and the intercalation of organic molecules and complexes in the interlayer of smectites.[25−28] As noted above, recent simulation studies by Titiloye and Skipper[5,6] have examined the structure and transport behavior of methane in smectite clay. Simulation of the intercalation of organic molecules within the interlayer of smectite typically requires the use of a hybrid energy force field that combines the parameters of the inorganic clay force field with those of the interaction parameters of the more conventional organic force field. We extend these previous intercalation simulations in the present study by using MD simulations to examine the structure and behavior of methane hydrate complexes in montmorillonite, a common smectite clay. In the next section, we first present the structural models and computational methods used in the simulation of the bulk structures of the methane hydrate and montmorillonite phases and then for the intercalated structures.

Methane Hydrate and Montmorillonite Unit Structures: The Building Blocks. Gas hydrates occur in several structural configurations depending primarily on the size of the guest molecule and the size of the internal cavity created by the coordinating H_2O water molecules.[29] Natural methane hydrates preferentially exist in the structure I configuration where H_2O molecules form cavities for hosting the guest methane molecules. The unit cell of the structure I hydrate crystallizes in the isometric system with 46 H_2O molecules forming two small spherical cavities (3.9 Å diameter with a H_2O coordination number of 20) and six large oblate cavities (∼4.3 Å diameter with a coordination number of 24). Approximately 70% of the cavities are occupied by methane molecules which hold the cavities apart to stabilize the structure. The molecular model of methane hydrate used here is based on the neutron diffraction structure of Hollander and Jeffrey[30] as determined for ethylene oxide hydrate. The methane hydrate unit cell was obtained by filling each of the eight cavities of the hydrate structure with methane molecules.[8] The unit cell was described by removing all constraints of internal symmetry such that the simulation cell has $P1$ symmetry. Larger simulation cells required for the bulk hydrate structure were created by expanding the unit cell in integral units. In contrast, however, simulations of the methane hydrate complex and the clay incorporated a single unit cell of the hydrate because of the observation that the

$d(001)$-value of ∼22 Å for the intercalate involves the 2:1 clay layer (9.8 Å) plus one unit cell (12 Å) of the methane hydrate complex.

Montmorillonite is a hydrated aluminosilicate comprised of layers, each layer formed by *one* central sheet composed of octahedrally coordinated Al atoms sandwiched between *two* opposing sheets of tetrahedrally coordinated Si atoms; hence, the descriptive terms of 2:1 or TOT layer. In the asymmetrical unit, three octahedral sites are available for metal occupancy but owing to charge balance only two of the three sites are occupied by Al, and thus montmorillonite is referred to as a dioctahedral structure. In montmorillonite, permanent layer charge is created primarily by substitution of divalent metals (e.g., Mg^{2+} and Fe^{2+}) for the octahedrally coordinated Al, creating a net negative charge on the 2:1 layer. Less common for montmorillonite is the substitution of Al for Si on the tetrahedral site. Hydroxyl groups form part of the coordination for each of the Al octahedra. The negative layer charge is balanced by interlayer exchangeable cations (e.g., Na^+, K^+, Ca^{2+}) that are easily hydrated by ambient H_2O which allows for the reversible expansion or contraction of the montmorillonite depending on the relative humidity.

A molecular model of Na-montmorillonite was developed from the structure of pyrophyllite,[21] which has no divalent metal cation substitution and thus no layer charge. Pyrophyllite is considered the dioctahedral endmember, and it has a stoichiometry of $Al_2Si_4O_{10}(OH)_2$ (with two asymmetric units per unit cell). Layer charge was introduced for the expanded unit cell $(2 \times 2 \times 1)$ by replacing selected octahedral Al with three Mg ions to obtain the most energetically favored magnesium distribution. The symmetry for the simulation cell was converted to $P1$ to accommodate the substitution and avoid any atomic constraints in subsequent simulations. No substitutions were made at the vacant octahedral site. Charge-balancing Na ions and associated H_2O molecules were added to the interlayer to produce a one-water-layer Na-pure montmorillonite structural model with a simulation cell composition of $Na_3(Mg_3Al_{13})$-$Si_{32}O_{80}(OH)_{16}\cdot16H_2O$. More detailed model descriptions are presented below.

Simulation Methods. Molecular simulations included the energy optimization of each structure followed by a series of isothermal and isobaric MD simulations. Each structure was treated as triclinic, $P1$ symmetry with periodic boundary conditions. Typically, all six cell parameters were allowed to vary independently. Additionally, all atomic positions were allowed to freely translate during the simulation. Interatomic potentials for the clay and H_2O components of the simulation cell were obtained from the *CLAYFF* force field developed by Cygan et al.[20] Each atom in the system has an assigned partial charge derived from quantum calculations and a set of Lennard-Jones parameters to characterize the short-range interaction behavior. The *CLAYFF* force field was originally developed for the simulation of various hydrated compounds and is based on the flexible simple-point-charge model for water and hydroxyl groups.[31,32] This approach provides for complete flexibility and relaxation of all system atoms and avoids the constraints required in most previous molecular simulations of clays.[24,33−35] This refinement also allows for conservation of energy and momentum across the solution−clay interface, thereby providing a more accurate description of interlayer sorption phenomena. Interatomic potentials for methane were taken from the *CVFF* force field of Dauber-Osguthorpe et al.[36] and include bond stretch and bond angle bend terms. The

Molecular Models

J. Phys. Chem. B, Vol. 108, No. 39, 2004 **15143**

Lennard-Jones parameters for the methane are compatible with those for those derived for the *CLAYFF* force field.

The total potential energy for the simulation cell is obtained by the summation of each contributing energy component:

$$E_{\text{Total}} = E_{\text{Coul}} + E_{\text{VDW}} + E_{\text{Bond Stretch}} + E_{\text{Angle Bend}} \quad (1)$$

where the long-range Coulombic energy is represented by

$$E_{\text{Coul}} = \frac{e^2}{4\pi\epsilon_o} \sum_{i \neq j} \frac{q_i q_j}{r_{ij}} \quad (2)$$

The partial charges q_i and q_j are derived from quantum mechanics calculations, e is the charge of the electron, ϵ_o is the dielectric permittivity of vacuum (8.85419×10^{-12} F/m), and r_{ij} is the distance between atoms i and j. The van der Waals energy E_{VDW} is represented by a Lennard-Jones function, and includes the short-range repulsion associated with the increase in energy, as two atoms approach each other, and the attractive dispersion energy:

$$E_{\text{VDW}} = \sum_{i \neq j} D_o \left[\left(\frac{R_o}{r_{ij}} \right)^{12} - 2 \left(\frac{R_o}{r_{ij}} \right)^6 \right] \quad (3)$$

D_o and R_o are empirical parameters derived from the fitting of the potential energy model to observed structural and physical property data. The $E_{\text{Bond Stretch}}$ and $E_{\text{Angle Bend}}$ terms in eq 1 include the energy represented by simple harmonic expressions for atomic configurations about an equilibrium bond distance (i.e., C–H bond for methane and O–H for H_2O and hydroxyl) and bond angle (i.e., H–C–H angle for methane and H–O–H angle for H_2O), respectively. The *CLAYFF* force field is parametrized to represent all clay component interactions, except for the H_2O and –OH groups, by the first two terms in eq 1.

The potential energy for each molecular model was evaluated with a spline cutoff distance of 8.5 Å for the nonbonded van der Waals interactions and an Ewald summation for the Coulombic interactions.[37,38] Energy minimization and MD simulations were performed with periodic boundary conditions and *P*1 symmetry allowing all atoms to have complete translational freedom. NPT ensemble MD simulations were performed at 1 atm and 300 K using the Nose–Hoover[39] and Parrinello–Rahman[40] methods to control temperature and pressure of the simulation, respectively. The Verlet[41] velocity algorithm was used to obtain accurate integrations and statistical ensembles. The MD time step was 0.001 ps for the bulk methane hydrate simulations and 0.0005 ps for those of the bulk montmorillonite and montmorillonite intercalate. Equilibrium configurations and energies were typically obtained within 10–20 ps of the simulation. MD simulations for the analysis of equilibrium structures and for deriving radial distribution functions were completed for times of either 50 or 100 ps in length. The methane hydrate, nominal Na-montmorillonite, Na-intercalate, and Ca-intercalate production simulations were run for 100 ps, whereas the K-intercalate and Mg-intercalate were completed for 50 ps. These production runs provided trajectory data that were collected every tenth time step. Additional MD simulations were performed to examine the solvation of methane in water (216 H_2O and periodic cell) and to examine an isolated methane within an expanded Na-montmorillonite (see below). All simulations were performed within the framework of the Cerius2 software package using the OFF energy code (Accelrys Inc., San Diego).
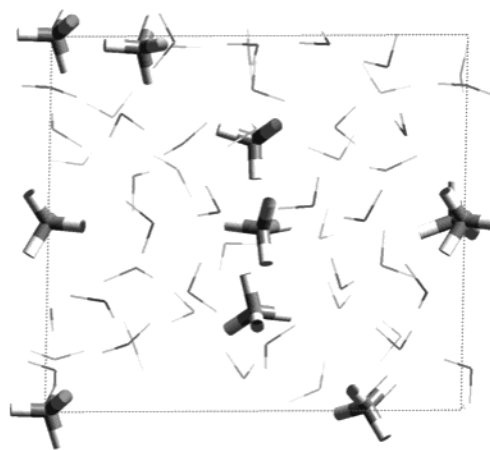

Figure 1. Unit cell structure for the methane gas hydrate obtained by energy minimization. Methane molecules represented by cylindrical C–H bonds and H_2O molecules by solid lines.

Results

Methane Hydrate Structure. The energy minimized configuration of the methane gas hydrate structure obtained at constant pressure conditions (Figure 1) exhibits a coordinated H_2O structure that is consistent with the experimental structure derived by Hollander and Jeffrey.[30] Methane molecules are maintained in the two different-sized cavities and exhibit various orientations on the basis of their initial configuration upon construction of the model. Slight distortion of the originally orthogonal system occurs depending on the methane orientations. An MD simulation of the expanded unit cell structure (2 × 2 × 2 supercell) provides a useful description of the hydrate structure. The larger simulation cell avoids constraints imposed by long-range order. Also, the flexibility of the H_2O and methane molecules are better examined by the dynamic equilibrium of the MD approach at ambient conditions rather than the static equilibrium—effectively a 0 K structure—determined by sampling of the potential energy surface through energy minimization procedures.

A snapshot of the equilibrated structure for the methane hydrate obtained from a 100 ps simulation at 300 K and 1 atm is presented in Figure 2. The dark dashed lines represent the hydrogen-bonding network associated with the H_2O molecules on the basis of a hydrogen bond distance less than 2.5 Å. This network is dynamic and reconstructs owing to the ability of the H_2O molecules to dynamically reorient themselves under the conditions of the simulation. The methane molecules freely reorient in the hydrate structure, with greater freedom to translate and rotate in the slightly larger oblate cavity. The H_2O–H_2O and H_2O–methane distances reported here are in very good agreement with those simulations reported previously.[16] Also, to our knowledge, our simulations represent the first fully flexible model for methane hydrate. The radial distribution functions (RDF) for the equilibrated methane hydrate are presented in Figure 3. The g(O–O) values are at a maximum at a distance of 2.73 Å and display a structure consistent with the recent simulations of Chialvo et al.[16] The carbon–carbon RDF has a maximum value at approximately 6.7 Å but also exhibits a fairly small and broad peak at 3.9 Å suggesting the occurrence of relatively strong methane–methane interactions across the structural cavities. The carbon–oxygen RDF peak occurs at 3.95 Å and is in excellent agreement with recent neutron diffraction results and pair correlation functions for methane hydrate.[42]
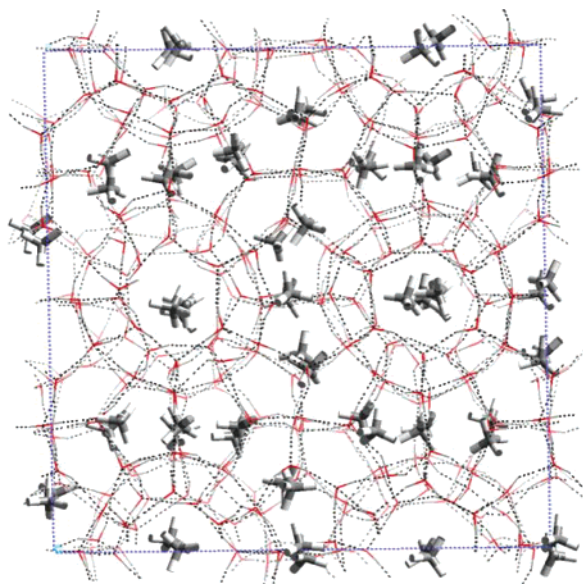
Figure 2. Snapshot of the equilibrated structure of 2 × 2 × 2 supercell of methane gas hydrate derived by MD simulation at 300 K and 1 atm after 100 ps. Hydrogen-bonding network among H_2O molecules is denoted by black dash lines. Color scheme: H_2O oxygens are red, H_2O hydrogens are light gray, methane hydrogens are light gray, and methane carbons are dark gray.
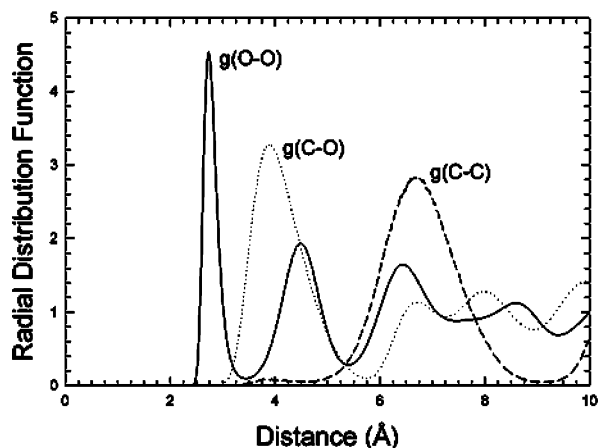

Figure 3. Radial distribution functions derived from the MD trajectories (300 K, 1 atm) for the methane hydrate.

Na-Montmorillonite Structure. The structure of the building-block Na-montmorillonite model is presented in Figure 4. This figure presents a representative structure from the equilibrated MD simulation completed at 300 K and 1 atm. The structure of the 2:1 layers, which include Mg-substituted octahedra and Al-substituted tetrahedra, is maintained throughout the simulation. Orientations of the hydroxyl groups in the 2:1 layer are affected by the vacant octahedral site and the Mg substitutions. Typically, the hydroxyls are oriented subparallel to the 2:1 layer, but they can be dynamically reoriented toward the interlayer depending on the disposition of the interlayer Na ions. The hydrated interlayer of montmorillonite is characterized by distribution of the H_2O molecules having their dipoles oriented so that the hydrogen atoms are nearest the surface of the 2:1 layers and the oxygen atoms point toward the central region of the interlayer, with approximately 62% directly interacting with the interlayer Na ions. Figure 5 provides the radial distribution functions $g(Na-O_{wat})$, $g(Na-O_{clay})$, and $g(O_{wat}-O_{wat})$. The two Na−O functions represent the solvation of the Na in the interlayer. Part of the oxygen coordination about
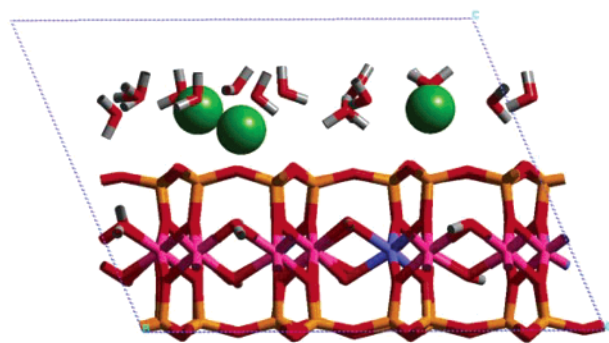

Figure 4. Snapshot of the equilibrated structure of the Na-montmorillonite building-block model derived by MD simulation at 300 K and 1 atm after 100 ps. Inner hydroxyls of the clay are typically pointing toward the vacant octahedral site, approximately normal to page. Color scheme: oxygens are red, hydrogens are gray, aluminums are magenta, magnesiums are blue, silicons are orange, and interlayer sodium ions are green spheres.
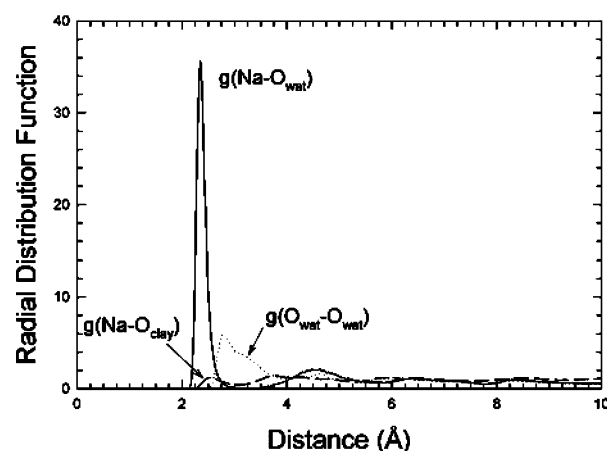

Figure 5. Radial distribution functions $g(Na-O_{wat})$, $g(Na-O_{clay})$, and $g(O_{wat-wat})$ derived from the MD trajectories (300 K, 1 atm) for the nominal Na-montmorillonite structure.

the sodium ion is that associated with the O_{clay} species. The Na−O distance at the peak maximum for the solvated ion in the interlayer is approximately 2.35 Å and is slightly smaller than the observed value of 2.41 Å for the aqueous octahedral solvation of sodium ion.[43] The primary peak value of 2.79 Å for $g(O_{wat}-O_{wat})$ agrees with recent experimental neutron data for oxygen−oxygen distances in (liquid) water.[44] This distance is increased slightly from the value observed for the methane hydrate and, most likely, is in response to the confined and restricted nature of the clay interlayer and the limited network of hydrogen bonding.

The mean basal $d(001)$-value for the Na-montmorillonite is 12.15 ± 0.14 Å. This swelling distance is in agreement with experiment[45] and with previous molecular simulation studies of clays.[46,47] Simulation of the dynamical behavior of interlayer H_2O is especially difficult owing to the large number of possible orientations that H_2O molecules can assume during a molecular mechanics optimization. In practice, it is impossible to sample all possible H_2O orientations by probing the potential energy surface, especially as the number of H_2O molecules in the simulation cell becomes excessive with the continued expansion of the clay with increasing H_2O content. We introduce pre-equilibrated H_2O volumes to the interlayer and initially perform energy minimization, but typically without meeting convergence criteria. However, subsequent MD simulation at ambient conditions provides an opportunity for dynamic equilibration of the

Molecular Models

J. Phys. Chem. B, Vol. 108, No. 39, 2004 **15145**

H_2O molecules. Another problem associated with clay simulations is the structural registry of the clay layers about the hydrated interlayer. As with other MD studies of clays that allow full relaxation,[18,20] we observe a shearing effect in the clay structure for long MD simulation times. This occasionally results in equilibrated clay structures with selected cell angles (α and β) being greatly distorted, but still providing accurate basal *d*-values and bulk structure.

Methane Hydrate Montmorillonite Intercalate Structures. The Na-montmorillonite structure was subsequently expanded to a supercell structure ($3 \times 2 \times 1$) with reduced symmetry (to *P*1) and an orthogonalized unit cell. The supercell structure is 3 times larger than that used by Park and Sposito[4] in their simulations of methane−montmorillonite systems. The supercell was equilibrated with additional interlayer H_2O to obtain a simulation cell of sufficient size to accommodate the unit-cell structure of the methane hydrate complex while avoiding potentially significant interactions of hydrates across periodic boundaries. The final Na-montmorillonite supercell is comprised of 2502 atoms with a formula stoichiometry of $Na_{18}(Mg_{18}Al_{78})$-$Si_{192}O_{480}(OH)_{96} \cdot 540 H_2O$.

Structures for the methane hydrate intercalate were created using the Na-montmorillonite supercell and the methane hydrate model. Initial simulations incorporated an anhydrous montmorillonite structure where all of the interlayer H_2O and Na were removed and replaced by several different-sized clusters derived from the methane hydrate unit cell. Finally, models of the full interlayer hydration of the methane hydrate were created by insertion of the $1 \times 1 \times 1$ cluster of the hydrate into the Na-montmorillonite simulation supercell with removal of the volume equivalent interlayer H_2O molecules, while still maintaining the interlayer Na. The hydrate cluster is comprised of 8 methane molecules and 46 H_2O molecules. We assume that each interlayer is occupied by the hydrate cluster, and the experimental data suggest that this is the case. Supercells for the K-, Ca-, and Mg-equivalent montmorillonites and intercalated hydrates were created directly from the Na-montmorillonite structures with subsequent equilibration simulations.

Various energy-optimized structures for the intercalated hydrate−clay system were obtained starting with the simple intercalation of the $1 \times 1 \times 1$ methane hydrate complex (involving H_2O and methane molecules) without any interlayer H_2O (hereafter referred to as "anhydrous" methane hydrate) in the expanded Na-montmorillonite (i.e., *d*(001)-value of 21.7 Å). The edge of the anhydrous methane hydrate was initially placed over a silicate hexagonal ring of the montmorillonite. The potential energy of the intercalate was monitored with each five-degree rotational increment from 0° to 90° of the hydrate, to examine the influence of the substrate positioning on the methane hydrate complex (cluster). The 2:1 layer and the methane hydrate were first held rigid and then allowed to fully relax with each new position. The results indicate only very small energy differences (approximately 30 kcal/mol for the complex or 0.01% of the total energy) among the structures, indicating that a methane hydrate complex can form at any angle to the underlying clay substrate.

An initial and equilibrated structure for the methane hydrate intercalated in the hydrated Na-montmorillonite is presented in Figure 6, as obtained after 5 and 100 ps of MD at 300 K and 1 atm. The models exhibit fully solvated Na ions about the preserved cluster of the methane hydrate. Although more-than-necessary simulation time is allotted to allow the diffusion of H_2O and methane molecules, and exchange of water between the hydrate cluster and the clay interlayer water, the simulation
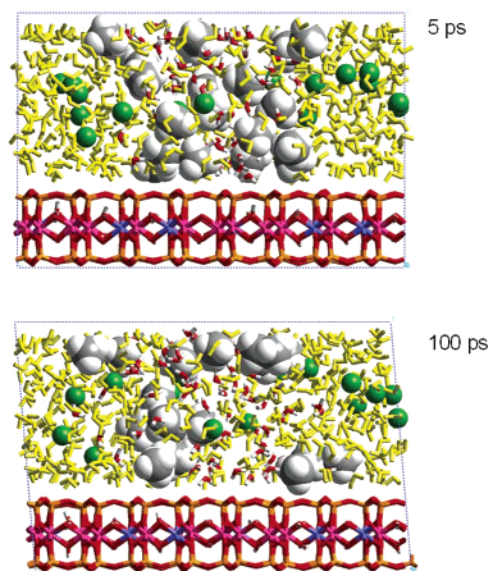

Figure 6. Snapshot of the structure of the fully hydrated methane hydrate intercalate with Na-montmorillonite as obtained by MD simulation at 300 K and 1 atm after 5 and 100 ps. The red-and-white-colored interlayer H_2O molecules represent those originally associated with the methane hydrate cluster; the remainder of the interlayer H_2O molecules are yellow; the interlayer sodium ions (spheres) are green. The light gray and dark gray colors represent, respectively, the hydrogen and carbon of the interlayer methane molecules. Color scheme for the clay: oxygens are red, hydrogens are white, aluminums are magenta, magnesiums are blue, and silicons are orange.
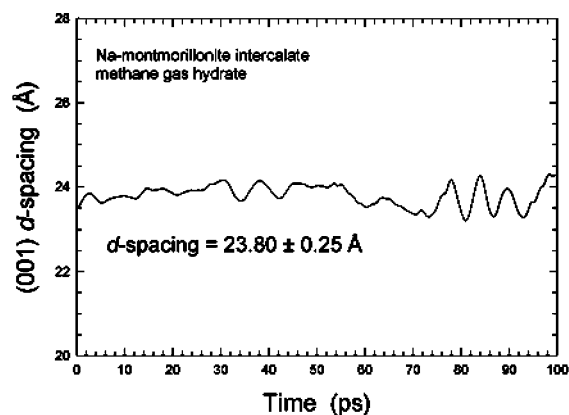

Figure 7. Basal *d*(001)-spacing for the equilibrated methane hydrate intercalate with Na-montmorillonite as a function of simulation time for the production run.

suggests some stabilization of the $1 \times 1 \times 1$ hydrate cluster within the interlayer of the montmorillonite resulting in a modified methane−water structure. Analysis of the simulation cell parameters indicates a mean basal *d*-value of 23.80 ± 0.25 Å for the equilibrated intercalate (see Figure 7), a value that is in general agreement with the ~22-Å peak from experiment.[1] An X-ray diffraction pattern for randomly oriented particles was calculated for the resulting intercalate structure; the pattern shows only two broad peaks at approximately 23.8 Å and 11.9 Å, which corresponds to the *d*(001) and *d*(002) basal diffractions. A similar analysis involving an MD simulation for the same methane hydrate intercalate, but run at 260 K and 1 atm, indicates a slightly smaller *d*-value of 23.53 ± 0.11 Å, a value not statistically different from that obtained for the 300 K simulation.

Similar intercalate structures were obtained for the montmorillonites with different interlayer cations of Ca^{2+}, K^+, and Mg^{2+}
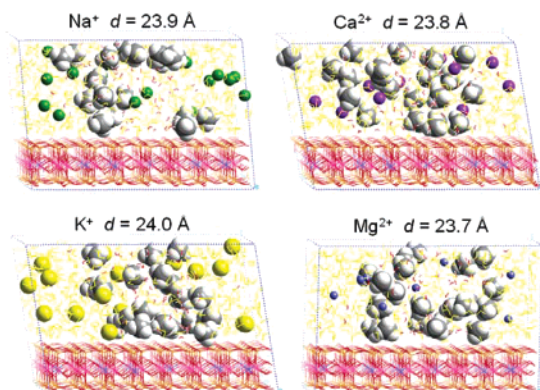
Figure 8. Comparison of the equilibrated methane hydrate intercalate structures for the different interlayer cations derived from MD simulations. Spheres representing interlayer cations are sized according to their ionic radii; sodiums are green, calciums are purple, potassiums are yellow, and magnesiums are blue. Color scheme for remaining atoms is the same as used for Figure 6.
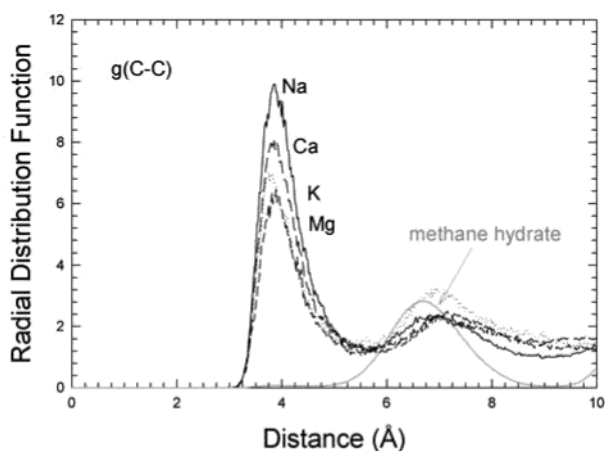

Figure 9. Radial distribution function $g(C_{meth}-C_{meth})$ derived from the MD trajectories for each of the four interlayer cations methane hydrate intercalates.

Figure 10. Radial distribution function $g(O_{wat}-O_{wat})$ derived from the MD trajectories for each of the four interlayer cations methane hydrate intercalates and for the bulk methane hydrate.

Figure 11. Radial distribution function $g(C_{meth}-O_{wat})$ derived from the MD trajectories for each of the four interlayer cations methane hydrate intercalates and for the bulk methane hydrate.

(Figure 8), instead of Na^+. The average basal *d*-values derived from the MD trajectories are similar, ranging from 23.74 Å for Mg^{2+} to 24.04 Å for K^+ with standard deviations of approximately 0.20 Å. There is no statistical difference in the expansion of the intercalated structure with interlayer cation. The radial distribution functions for C−C distances for the methane molecules are presented in Figure 9. This plot provides a measure of the coherency of the methane hydrate cluster within the interlayer. All four structures exhibit similar methane−methane distances including a secondary peak maximum at approximately 6.8 Å which is consistent, although slightly higher, than observed at 6.7 Å for the bulk methane hydrate. However, the major peak at 3.9 Å for each intercalate indicates the presence of significant methane−methane interactions within the clay. The 3.9 Å peak is coincident with the small C−C peak (see Figure 3) observed for the bulk methane hydrate.

Other measures of the interlayer structure for the methane hydrate in montmorillonite are provided by the $g(O_{wat}-O_{wat})$ and $g(C_{meth}-O_{wat})$ radial distribution functions (Figures 10 and 11) where all interlayer H_2O molecules are included in the calculation. Each of the four compositions of the intercalate exhibit equivalent oxygen−oxygen distances for the primary peak region at 2.7 Å in agreement with the main peak associated with bulk methane hydrate. However, the distribution functions for the intercalates broaden considerably at greater distances
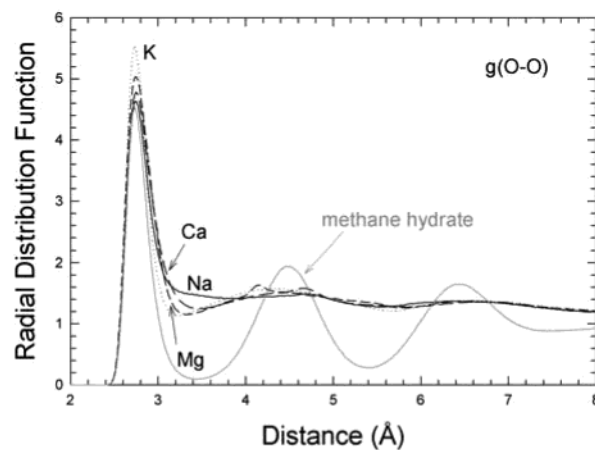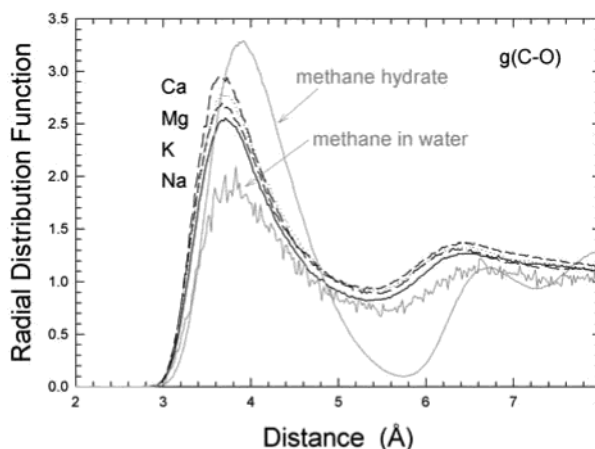
relative to the 4.5 Å and 6.4 Å peaks observed for the methane hydrate. Thus, the H_2O molecules associated with the methane preserve only limited local order after intercalation. The carbon−oxygen distribution functions derived for each of the four interlayer metal montmorillonite compositions exhibit nearly equivalent behavior. They show a primary peak at approximately 3.7 Å and a secondary peak at 6.4 Å. Both peaks are shifted to smaller values relative to those observed in the RDFs derived for the simulated bulk methane hydrate and those obtained from neutron diffraction experiments.[42] Additionally, the major peak for the intercalate systems exhibits a narrower distribution than that derived for the methane hydrate. The 3.7 Å peak is consistent with that observed in the C−O RDF derived from an MD simulation of the aqueous solvation of methane (300 K and 1 atm) and is similar to those derived in other theoretical studies.[2,48]

Discussion

Most deliberate in the present study is our emphasis on the behavior of methane hydrate in an expanded montmorillonite clay structure. MD simulations were performed using an initially ordered methane hydrate complex appropriately sized to an expanded montmorillonite (approximate basal *d*-values of 23 Å to 24 Å). This contrasts with previous theoretical studies where either a two-layer hydrate[3,5,6] or three-layer hydrate[4] of
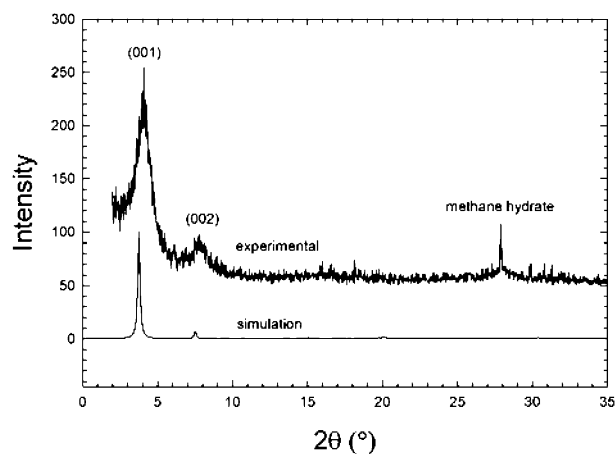
Molecular Models

J. Phys. Chem. B, Vol. 108, No. 39, 2004 **15147**

Figure 12. Comparison of the experimental[1] and simulated X-ray diffraction patterns for the methane hydrate intercalate. The 28° 2θ peak for the experimental data is related to the incipient growth of methane hydrate in association with the intercalated phase.

Na-montmorillonite was simulated to evaluate the coordination and transport behavior of a limited number of methane molecules within the interlayer. Our MD results demonstrate a stabilization of the methane hydrate intercalate in the expanded montmorillonite structure corresponding to approximately five to six water layers, some of which exhibit some ordering within the methane hydrate component and some disordered within the hydrated montmorillonite. These results are in general agreement with the methane hydrate intercalate structure inferred from the X-ray diffraction analysis of synthesized material.[1]

A comparison of X-ray diffraction patterns is presented in Figure 12 where a simulated diffraction pattern derived from one of the theoretical structures of the methane hydrate intercalate is compared with an experimental structure. The simulated diffraction pattern was derived assuming a random distribution of particles with no preferred orientation. We selected a representative MD structure from the 100 ps production trajectory for the methane hydrate in Na-montmorillonite run at 260 K and 1 atm. The experimental diffraction pattern was obtained in situ for a sample equilibrated at 267 K and 41 atm methane pressure for 126 h. As noted previously, we do not observe significant structural changes in the intercalate between the 260 and 300 K MD simulations, nor would differences be expected for these relatively small pressure differences, especially as temperature and pressure are not precisely controlled in the simulations;[37] we observe variations of approximately 15 K and 150 MPa (1500 atm) for temperature and pressure, respectively. Both diffraction patterns are dominated by the low-angle peaks (~4° and ~7.5° 2θ) representing the basal plane reflections (001, 002) of the montmorillonite methane hydrate. The 2θ values correspond to d-spacings of approximately 22 Å for the experimental data and 23.5 Å for the simulation, and approximately 11 Å and 11.7 Å, respectively, for the 002 peak. Evidence of a crystallized methane hydrate also occurs in the experimental pattern at approximately 27° 2θ and is inferred to be associated with the incipient growth of the methane hydrate in the sample after long equilibration times.[1] Little diffraction information is observed in both experiment and simulation at higher 2θ values owing to the lack of long-range order of the intercalate structure. Because the experimental pattern involves a high degree of preferred orientation and the calculated pattern is based on a random distribution of particles, it is likely that little additional information will be obtained by designing experiments where grains have no preferred orientation.

Our molecular simulations indicate that methane occurs in the interlayer of the montmorillonite in one of three general configurations: (1) coordinated by H_2O within a quasi-stable methane hydrate cluster; (2) coordinated to the siloxane surface of the clay and the H_2O associated with the methane hydrate cluster; and (3) coordinated by H_2O after diffusing from the methane hydrate cluster. The methane that remains coordinated by H_2O within the original cluster does not preserve the relatively ordered structure of the methane hydrate. Our results suggest a disordering of the cluster as indicated by the shift of the carbon–oxygen RDF peak to shorter differences and to a more water-like environment (Figure 11). The narrowing of this peak and that of the carbon–carbon RDF (Figure 9) relative to the bulk methane hydrate is representative of the collapse of the two types of cavities characteristic of the bulk phase. Methane is significantly more dynamic by moving (translations and rotations) about the cavities in the bulk phase than by being fully solvated by H_2O within the interlayer.

Methane in the second configuration is coordinated in part by the relatively hydrophilic surface of the montmorillonite and is positioned over the central part of the hexagonal rings that comprise the predominantly Si–O network. This results in a relatively stable cage-like configuration with 6–8 oxygen atoms of the tetrahedra sheet and roughly 10 to 12 H_2O molecules coordinated about the methane molecule (total coordination number of 16–20). The variation in coordination is related to the dynamical aspect of the simulation and the local mobility of the methane within the clathrate-like cage. Carbon–oxygen distances range from approximately 3.2 Å to 4.9 Å (distances representing the entire interlayer region can be compared in Figure 11). This methane coordination is very similar to the small spherical cavity of the structure I hydrate[30] and is in agreement with the coordination observed in the neutron diffraction study of de Jong et al.[49] for hydrated methane. The observations are consistent with the simulations of Titiloye and Skipper[5] and Park and Sposito[4] but are distinguished by somewhat less H_2O involved in this coordination owing to the competition of the H_2O with the other methane molecules of the methane hydrate cluster. Equivalent results for methane coordination were found for each of the four different montmorillonite compositions.

We examined the stability of an isolated methane in a clay surface configuration by performing an MD simulation of the expanded 23 Å montmorillonite (approximately six H_2O layers) with a single methane molecule. The methane remains stable as an inner sphere complex above the hexagonal ring throughout the 100 ps simulation. One would expect the nonpolar methane to have less affinity to the montmorillonite surface relative to the polar H_2O molecule. Differences in nonbonded interactions for methane–clay and H_2O–clay surfaces support this argument on the basis of the partial charge assignments for methane and H_2O and the relative strength of their Coulombic interactions with the clay surface. However, the MD simulation shows the formation of a crown of 14–16 H_2O molecules about the methane (total coordination number of 20–22) and the formation of a stable hydrogen-bonding network among the coordinating H_2O molecules and the methane. An energy stabilization of approximately 3 kcal/mol would be gained for each hydrogen bond formed between H_2O molecules and significantly less stabilization for those forming between H_2O and methane. This result is consistent with our calculations for the sorbed methane of the methane hydrate intercalate where we observe a slightly lower coordination number for the clathrate. A related

simulation was performed for an isolated methane but with only a three-layer hydrate of Na-montmorillonite.

The third environment for methane within the intercalate involves an isolated methane molecule, solvated by interlayer H_2O, and which is no longer associated with the methane hydrate cluster. Figure 8 includes several examples of methane diffusion within the clay interlayer. We observe this behavior for only methane molecules that occur on the edge surfaces of the original methane hydrate cluster and have the capability to migrate from the cluster. The methanes on the top and bottom of the cluster are effectively fixed by the montmorillonite surface. Computational limitations prevented us for from quantifying the diffusion rates. We also observe the dynamic behavior of the interlayer metal cations for each of the montmorillonite compositions. Each metal remains fully solvated by H_2O and in a few occasions, particularly for K^+, dynamically diffuses and sorbs directly to the montmorillonite surface to form a stable inner sphere (see Figure 8). This behavior is not unexpected owing to the low hydration energy associated with K^+ relative to the other metal cations.[50] For each of the simulations, we do not observe methane in coordination with the interlayer metals. We interpret this behavior to be related to the high energy cost of replacing a polar H_2O with a nonpolar methane, but this may occur for high methane content.[3]

We suggest that the montmorillonite 2:1 layer surface provides a stabilizing influence on the formation of methane clathrate complexes. This conclusion is based on simulations (those presented here and elsewhere)[3-6] and on experimental data[1], which also suggest that with higher methane content, a methane-hydrate-like complex can exist within the montmorillonite interlayer having both interlayer surfaces stabilize the complex. The simulations presented here are in agreement with the experimental data involving a significantly expanded interlayer. Assuming that temperature (-10 °C to 10 °C) and pressure (20–60 atm) conditions exist for thermodynamic stability of the bulk methane hydrate, it is not difficult to envision that some form of the ordered hydrate will exist after intercalation into the clay. Although we do not observe the same level of ordering for the intercalate as observed for the crystalline methane hydrate, there is some structure preserved for up to 200 ps simulation time. Methane molecules maintain an association of H_2O molecules within the interlayer resulting in a dynamic network of hydrogen bonding among H_2O and methane molecules extending from one side of the interlayer to the other. This network is pinned to the montmorillonite by stable methane–H_2O clathrate structures that form on each siloxane surface.

Conclusions

We have presented molecular simulations of the structure and behavior of methane and H_2O in the interlayer of an expanded montmorillonite clay. Particular emphasis was placed on the analysis of a modified methane hydrate cluster within an expanded interlayer of the montmorillonite initially comprised of five to six H_2O layers. The results provide a theoretical basis to support the recent experimental observations[1,2] relating to the influence of 2:1 clay minerals and the stability of methane hydrate and methane hydrate intercalates. The MD model indicates that a methane-hydrate-like complex is stable within the montmorillonite interlayer and produces a d(001)-value for the intercalate that is consistent with experimental observation. The large-scale simulations allow full atomic flexibility and provide a basis for future studies involving various H_2O–methane compositions. It would be of particular interest to expand the present study to examine the hydration enthalpies of the methane hydrate intercalate as a function of methane composition, especially with regards to the stability of any methane–water structure within the montmorillonite interlayer. Because it is unlikely that a crystallographically unreasonable structure will crystallize, molecular modeling techniques provide useful information about the viability of various possible structures. However, a crystallographically reasonable structure obtained by modeling does not inform about the viability of crystallization, because of the lack of data about kinetic effects. For montmorillonite with various interlayer cations, it is necessary to have substantial and accessible interlayer H_2O to provide the framework for guest molecules, such as methane, for the hydrate complex. The modeling here assumes that the interlayer contains sufficient interlayer H_2O regardless of the interlayer cation type.

References and Notes

(1) Guggenheim, S.; Koster van Groos, A. F. *Geology* **2003**, *31*, 653.

(2) Cha, S. B.; Ouar, H.; Wildeman, T. R.; Sloan, E. D. *J. Phys. Chem.* **1988**, *92*, 6492.

(3) Gist, G. A. *Molecular models of methane absorption in smectite clay*; Exxon Mobil Upstream Research Co.: Houston, TX, 2000.

(4) Park, S.-H.; Sposito, G. *J. Phys. Chem. B* **2003**, *107*, 2281.

(5) Titiloye, J. O.; Skipper, N. T. *Mol. Phys.* **2001**, *99*, 899.

(6) Titiloye, J. O.; Skipper, N. T. *Chem. Phys. Lett.* **2000**, *329*, 23.

(7) Jager, M. D.; Sloan, E. D. *Fluid Phase Equilib.* **2001**, *185*, 89.

(8) Hirai, H.; Kondo, T.; Hasegawa, M.; Yagi, T.; Yamamoto, Y.; Komai, T.; Nagashima, K.; Sakashita, M.; Fujihisa, H.; Aoki, K. *J. Phys. Chem. B* **2000**, *104*, 1429.

(9) Ahlrichs, J. L.; White, J. L. *Science* **1962**, *136*, 1116.

(10) Anderson, D. M.; Morgenstern, N. R. Physics, chemistry, and mechanics of frozen ground: A review. In *North American Contributions to Permafrost*; National Academy of Sciences: Washington, DC, 1973; p 257.

(11) Rodger, P. M. *AIChE J.* **1991**, *37*, 1511.

(12) Rodger, P. M.; Forester, T. R.; Smith, W. *Fluid Phase Equilib.* **1996**, *116*, 326.

(13) Hwang, M. J.; Holder, G. D.; Zele, S. R. *Fluid Phase Equilib.* **1993**, *83*, 437.

(14) Forrisdahl, O. K.; Kvamme, B.; Haymet, A. D. J. *Mol. Phys.* **1996**, *89*, 819.

(15) Zele, S. R.; Lee, S. Y.; Holder, G. D. *J. Phys. Chem. B* **1999**, *103*, 10250.

(16) Chialvo, A. A.; Houssa, M.; Cummings, P. T. *J. Phys. Chem. B* **2002**, *106*, 442.

(17) van der Waals, J. H.; Platteeuw, J. C. *Adv. Chem. Phys.* **1959**, *2*, 1.

(18) Teppen, B. J.; Rasmussen, K.; Bertsch, P. M.; Miller, D. M.; Schäfer, L. *J. Phys. Chem.* **1997**, *B101*, 1579.

(19) Sainz-Diaz, C. I.; Hernández-Laguna, A.; Dove, M. T. *Phys. Chem. Miner.* **2001**, *28*, 130.

(20) Cygan, R. T.; Liang, J.-J.; Kalinichev, A. G. *J. Phys. Chem. B* **2004**, *108*, 1255.

(21) Lee, J. H.; Guggenheim, S. *Am. Mineral.* **1981**, *66*, 350.

(22) Bish, D. L. *Clays Clay Miner.* **1993**, *41*, 783.

(23) Boek, E. S. *Langmuir* **1995**, *11*, 4629.

(24) Smith, D. E. *Langmuir* **1998**, *14*, 5959.

(25) Hartzell, C. J.; Cygan, R. T.; Nagy, K. L. *J. Phys. Chem. A* **1998**, *102*, 6722.

(26) Teppen, B. J.; Yu, C.; Miller, D. M.; Schäfer, L. *J. Comput. Chem.* **1998**, *19*, 144.

(27) Yu, C. H.; Newton, S. Q.; Miller, D. M.; Schäfer, L.; Teppen, B. J. *Clays Clay Miner.* **2000**, *48*, 665.

Molecular Models

J. Phys. Chem. B, Vol. 108, No. 39, 2004 **15149**

(28) Yu, C. H.; Norman, M. A.; Newton, S. Q.; Miller, D. M.; Teppen, B. J.; Schäfer, L. *J. Mol. Struct.* **2000**, *556*, 95.

(29) Sloan, E. D. *Clathrate Hydrates Natural Gases*, 2nd ed.; M. Dekker: New York, 1998.

(30) Hollander, F.; Jeffrey, G. A. *J. Chem. Phys.* **1977**, *66*, 4699.

(31) Berendsen, H. J. C.; Postma, J. P. M.; van Gunsteren, W. F.; Hermans, J. Interaction models for water in relation to protein hydration. In *Intermolecular Forces*; Pullman, B., Ed.; D. Reidel: Amsterdam, 1981; p 331.

(32) Teleman, O.; Jonsson, B.; Engstrom, S. *Mol. Phys.* **1987**, *60*, 193.

(33) Skipper, N. T.; Refson, K.; McConnell, J. D. C. *Clay Miner.* **1989**, *24*, 411.

(34) Chang, F. C.; Skipper, N. T.; Sposito, G. *Langmuir* **1995**, *11*, 2734.

(35) Greathouse, J. A.; Refson, K.; Sposito, G. *J. Am. Chem. Soc.* **2000**, *122*, 11459.

(36) Dauber-Osguthorpe, P.; Roberts, V. A.; Osguthorpe, D. J.; Wolff, J.; Genest, M.; Hagler, A. T. *Proteins: Struct. Funct. Genet.* **1988**, *4*, 31.

(37) Allen, M. P.; Tildesley, D. J. *Computer Simulation of Liquids*; Oxford University Press: New York, 1987.

(38) Tosi, M. P. *Solid State Phys.* **1964**, *131*, 533.

(39) Hoover, W. G. *Phys. Rev. A* **1985**, *31*, 1695.

(40) Parrinello, M.; Rahman, A. *J. Appl. Phys.* **1981**, *52*, 7182.

(41) Verlet, L. *Phys. Rev.* **1967**, *159*, 98.

(42) Koh, C. A.; Wisbey, R. P.; Wu, X. P.; Westacott, R. E.; Soper, A. K. *J. Chem. Phys.* **2000**, *113*, 6390.

(43) Caminiti, R.; Licheri, G.; Piccaluga, G.; Pinna, G. *Chem. Phys. Lett.* **1977**, *47*, 275.

(44) Soper, A. K. *Chem. Phys.* **2000**, *258*, 121.

(45) Fu, M. H.; Zhang, Z. Z.; Low, P. F. *Clays Clay Miner.* **1990**, *38*, 485.

(46) Young, D. A.; Smith, D. E. *J. Phys. Chem. B* **2000**, *104*, 9163.

(47) Cygan, R. T. Molecular modeling in mineralogy and geochemistry. In *Reviews in Mineralogy and Geochemistry: Molecular Modeling Theory: Applications in the Geosciences*; Cygan, R. T., Kubicki, J. D., Eds.; The Geochemical Society: Washington, D.C, 2001; p 1.

(48) Guillot, B.; Guissani, Y. *J. Chem. Phys.* **1993**, *99*, 8075.

(49) de Jong, P. H. K.; WIlson, J. E.; Neilson, G. W.; Buckingham, A. D. *Mol. Phys.* **1997**, *91*, 99.

(50) Tanaka, N.; Ohtaki, H.; Tamanushi, R. *Ions and Molecules in Solution*; Elsevier: Amsterdam, 1983.